ACS APPLIED MATERIALS & INTERFACES

RESEARCH ARTICLE

www.acsami.org

Effect of Genipin Crosslinking on the Optical Spectral Properties and Structures of Collagen Hydrogels

Yu-Jer Hwang,[†] Jillian Larsen,[‡] Tatiana B. Krasieva,[§] and Julia G. Lyubovitsky*[,‡]

[†]Cell Molecular and Developmental Biology Program (CMBD) and [‡]Department of Bioengineering, University of California Riverside, Riverside, California 9252

[§]Beckman Laser Institute, University of California Irvine, Irvine, California 92602

Supporting Information

ABSTRACT: Genipin, a natural cross-linking reagent extracted from the fruits of *Gardenia jasminoides*, can be effectively employed in tissue engineering applications due to its low cytotoxicity and high biocompatibility. The cross-linking of collagen hydrogels with genipin was followed with one-photon fluorescence spectroscopy, second harmonic generation, fluorescence and transmission electron microscopy. The incubation with genipin induced strong auto-fluorescence within the collagen hydrogels. The fluorescence emission maximum of the fluorescent adducts formed by genipin exhibit a strong dependence on the excitation wavelength. The emission maximum is at 630 nm when we excite the cross-linked samples with 590 nm light and shifts to 462 nm when we use 400 nm light instead. The fluorescence imaging studies show that genipin induces formation of long aggregated fluorescent strands throughout the depth of samples. The second harmonic generation (SHG) imaging studies suggest that genipin partially disaggregates 10 μm "fiberlike" collagen structures because of the formation of these fluorescent cross-links. Transmission electron microscopy (TEM) studies reveal that genipin largely eliminates collagen's characteristic native fibrillar striations. Our study is the first one to nondestructively follow and identify the structure within collagen hydrogels in situ and to sample structures formed on both micro- and nanoscales. Our findings suggest that genipin cross-linking of collagen follows a complex mechanism and this compound modifies the structure within the collagen hydrogels in both micro- and nanoscale.

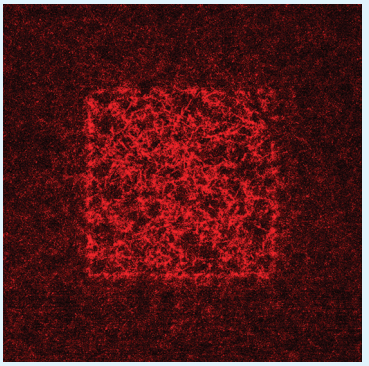

KEYWORDS: collagen, hydrogel, genipin, crosslinking, structure, second harmonic generation

INTRODUCTION

The cross-linking of collagen-based scaffolds/gels is often employed to strengthen them for tissue engineering applications. The effects of these processes on collagen structures in both micro and nano-scales as well as the induced optical properties are usually not systematically investigated. To clarify the effects of cross-linking on biologically derived scaffolds, it is critical to characterize these structure−function relationships.

This study investigates the effects of genipin cross-linking on the structure and optical properties of three-dimensional (3D) collagen hydrogels. Specifically, the study is set to answer a question if genipin crosslinking modifies the nano- and micro- structures of collagen as well as establishing for the first time a combination of methods to follow this process in situ and in real time. This was achieved through examining the genipin cross-linked collagen hydrogels with one-photon fluorescence spectroscopy, evaluating the kinetics of fluorescence production in the gels undergoing the cross-linking reaction, application of second harmonic generation, fluorescence and transmission electron microscopy to evaluate changes in micro- and nanostrucutures. The data and methods developed provide an outline to monitor in situ the extent of cross-linking of collagen hydrogels with genipin.

Genipin compound is an iridoid derivative isolated from the fruits of *Gardenia jasminoides*. It generates both color and fluorescence in a single reaction with biopolymers containing primary amine groups. The reaction between genipin and collagen induces the formation of cyclic structures, which serve as the intramolecular and intermolecular crosslinks between collagen molecules within fibers.[1] To date, genipin found practical use as a bioadhesive,[2] amino acid[3] and fingerprint[4,5] detection reagent. Additionally, it had been employed to cross-link various hydrogels for biomaterial,[6,7] drug delivery applications,[8] and preparation of porous constructs.[9]

An important feature of the collagen biopolymer is that collagen within it is self-assembled into the structural elements ranging from angstroms to micrometers and larger dimensions. Specifically, triple-helical collagen molecules are packed together into the staggered patterns called fibrils, which are the nanostructures routinely studied with transmission electron microscopy (TEM). Higher-order microstructural bundles of collagen fibrils within the hydrogels that are called fibers can be effectively investigated deep within materials with nondestructive laser-scanning optical methods such as confocal and multiphoton microscopy (MPM).[10,11] Briefly, MPM imaging utilizes femtosecond pulses of near-infrared (NIR) laser light and can generate

Received: April 5, 2011
Accepted: June 6, 2011
Published: June 06, 2011

high resolution and contrast three-dimensional images of biological samples. Its advantages include reduced scattering because NIR wavelengths are employed, no out-of focus absorption, very small sample volumes and deeper tissue penetration compared to confocal microscopy.[12] The interaction between fibrillar collagen and NIR pulsed, femtosecond laser light of MPM has been identified to result in second harmonic generation (SHG), which is produced when photons interacting with fibrillar collagen are combined to form new photons with exactly twice the energy.[13] SHG gained recognition in tissue imaging[11,13−21] because this source of contrast resists photobleaching and had been used to successfully image structural proteins in various non-animal and animal sources[22] with strong enhancement suitable for biomedical assessment of tissue structure.[20] The interaction between laser pulses and collagen's non-centrosymmetric, triple helix structure in addition to molecular packing within collagen materials leads to scattering from the tertiary (fibrils),[20] and quaternary (fibers),[1323] thus producing SHG.[24] The intrinsic fluorescence is generated by UV/VIS absorbing molecular structures and proteins. The cross-linking products formed by genipin when it reacts with biopolymers containing primary amine groups are known to absorb in the mid-UV (250−300 nm),[25] near-UV (320−370 nm),[6] visible wavelength range (400−600 nm),[26] and fluoresce in the 380−700 nm wavelength region.

EXPERIMENTAL SECTION

Collagen Materials Formation and Cross-Linking. Soluble rat-tail type I collagen, 9.58 mg/mL (BD Biosciences) was in 0.02 N acetic acid. The purity of this stock solution was verified with 4%-20% Tris-HCl gels (Bio-Rad) following a standard protocol. The stock solution was diluted with 0.02 N acetic acid to obtain the 2X collagen aliquots. 2X initiation buffers were prepared from NaCl and phosphate buffer. The concentration of mono-and dibasic phosphate in the buffer at pH 7.4 were calculated with Henderson-Hasselbalch equation. The pH was adjusted drop-wise with 1N NaOH or HCl. Ionic strength was adjusted with NaCl. The initiation buffer had the following components: 6.40 g/L K_2HPO_4; 3.16 g/L KH_2PO_4; 38.55 g/L NaCl (ionic strength = n0.6 M). After the pH was adjusted to a desired value, the initiation buffer were filtered with 0.22 μm, 25 mm syringe filter (Fisher) and stored at 4 °C. Prior to the beginning of material formation, both 2X collagen stock and initiation buffer were de-airated by placing in a 1.5 L desiccator (Fisher) and applying house vacuum for 2 h. Material formation was initiated by mixing 2× collagen aliquot with 2× initiation buffer on ice at 1:1 ratio, verifying the pH to be 7.4 ± 0.1, and then incubated at 37 °C. The final collagen concentration of the materials is 2 mg/mL. For multi-photon microscopy and confocal microscopy measurements collagen materials were prepared in 8-well chambered coverglass (MP Biomedicals). For one-photon experiments collagen materials were prepared in 96-well plates (BD Falcon). In both cases, after 24 h incubation at 37 °C, the materials were incubated in 1 or 10 mM genipin solutions (Sigma) at the same temperature for the specified times.

Fluorescence Measurements. Increase in fluorescence intensity within the materials that was due to genipin cross-linking was measured in situ, in a high-throughput format using a FlexStation microplate reader in a backscattering mode (Molecular Devices). The excitation wavelength was 590 nm and emission spectrum was collected from 620 to 760 nm. Additional fluorescence spectra were obtained for different excitation wavelengths as shown in the Supporting Information, Figure S1. Measurements were taken on the same samples every 1 h during the first 9 h and subsequently 2 measurements every 24 h. Per one experimental run, a spectrum was independently acquired from two wells. The background fluorescence was subtracted from each spectrum, and the spectra were averaged. All experimental runs were repeated on different days and up to three times using identical settings for the measurements. The error bars are standard deviations from the mean. After the fluorescence intensity reached the plateau, cross-linked samples were shaken thoroughly in a 0.3 M ionic strength phosphate buffer (NaCl added to adjust ionic strength) to remove the unreacted genipin.

Multiphoton Microscopy (MPM) and Confocal Microscopy. The inverted multiphoton laser scanning microscope used in this work was the Zeiss LSM 510 NLO Meta microscopy system. It is based on an Axiovert 200M inverted microscope equipped with standard illumination systems for transmitted light and epi-fluorescence detection. It was also equipped with an NLO interface for a femtosecond titanium: sapphire laser excitation source (Chameleon-Ultra, Coherent, Incorporated, Santa Clara, CA) for multiphoton excitation. The Chameleon laser provided femtosecond pulses at a repetition rate of about 80 MHz, with the center frequency tunable from 690 to 1040 nm. A Helium−Neon 543 nm laser was also equipped for confocal excitation. A long working distance objective (Zeiss, 40x water, N.A. 0.8) was used to acquire images shown in this work. The signals from the samples were epi-collected and discriminated by the band pass 700/543 nm dichroic beamsplitter for fluorescence imaging and by the short pass 650 nm dichroic beamsplitter for SHG imaging. The SHG images were collected with the 394−405 nm band-pass filter (λ_{ex} = 800 nm). The fluorescent images were collected with the 565−615 nm band-pass filter (λ_{ex} = 543 nm). Each image presented in this work is 12 bit, 512 × 512 pixels representing 225 μm × 225 μm field of view. All the images were repeated on separate days, using up to 8 independent samples on each day (about 5 fields of view per sample).

Transmission Electron Microscopy (TEM) Imaging. After 24 h of incubation, entire portion of an incubated sample was retrieved. A drop of sample containing cross-linked material was added on a formvar film coated with a layer of carbon supported on a 300-mesh copper grid (Carbon type A, Ted Pella, Inc.). Excess liquid was drained with filter paper after 30 s. A drop of double de-ionized water was then added to the sample on the grid for 1 s to remove the excess NaCl, and was drained slowly with filter paper. A drop of same-day-prepared 1 g/L sodium phosphotungstate (Sigma), pH 7.4 was added to the sample on the grid. After 10 minutes of staining, the grid was drained slowly with filter paper and then air-dried for about 15 minutes. The grids were examined immediately in a Tecnail 12 electron microscope operated at 120 kV.

RESULTS AND DISCUSSION

Two potential molecular mechanisms for genipin modification of biopolymers containing primary amine groups are described in literature.[26,27] For collagen, they are schematically shown in Figure 1. The first cross-linking pathway begins with a nucleophilic attack of the collagen's primary amine of lysine, hydroxylysine and arginine residues on the genipin C3 carbon to form a nitrogen-iridoid.[28] Subsequently, the tertiary nitrogen of collagen replaces an oxygen atom in the genipin's six-membered ring. The intramolecular and intermolecular crosslinks formed are the linked cyclic structures of nitrogen substituted genipin attached to collagen.[29] Two iridoids subsequently dimerize through a radical reaction (Figure 1A).[2] The second proposed pathway starts with a nucleophilic substitution reaction that replaces the ester group of genipin by a secondary amide linkage.[27] The final product for this second possible pathway is unknown.

In situ One-Photon Fluorescence Characterization of Genipin Cross-Linked Collagen Hydrogels. In general, the reaction of genipin compound with primary amines in amino acids produces a stable blue pigment with exact color being determined by the type of the reacting amino acid.[30] When we treat the initially semi-translucent collagen hydrogels with a clear solution of 1 mM or 10 mM genipin, their color gradually becomes red-purple within a few days due to the progress of

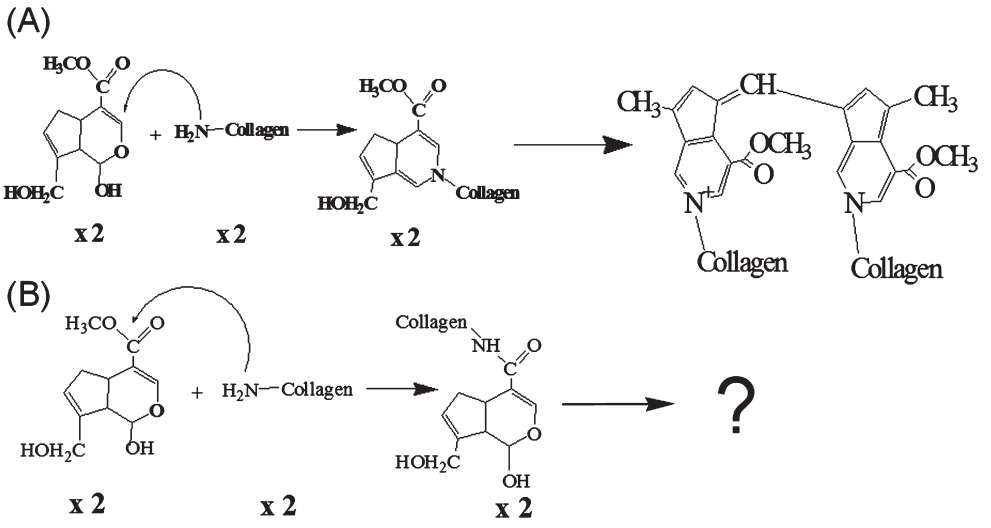

Figure 1. Schematics for the cross-linking reactions of collagen with a genipin compound.

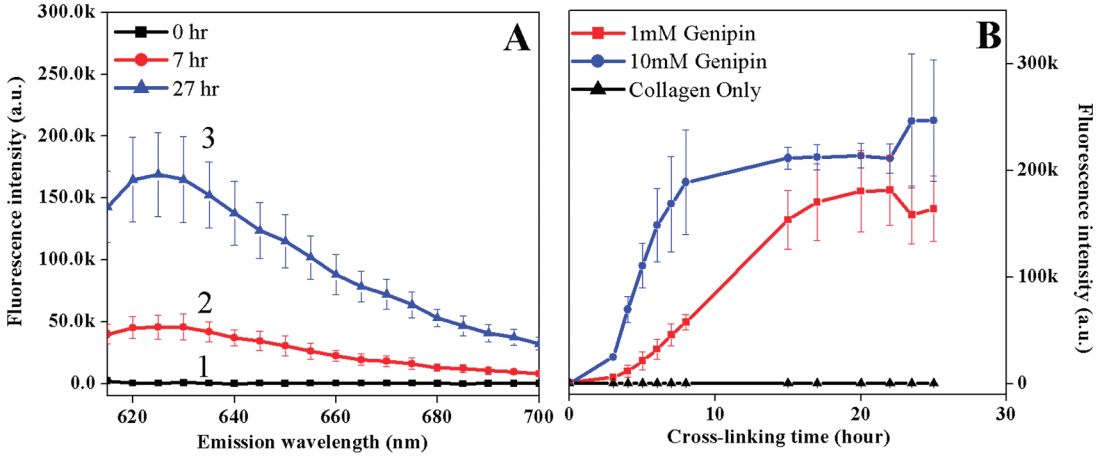

Figure 2. Effect of genipin cross-linking on the production of fluorophores (λ_{ex} = 590 nm): (A) Typical in situ fluorescence emission spectra of the collagen hydrogels incubated with genipin for 0 h (1), 7 h (2), and 27 h (3). The data shown are for 1 mM genipin. (B) Fluorescence intensity ($\lambda_{ex}/\lambda_{em}$ = 590 nm/630 nm) as a function of cross-linking time for collagen hydrogels incubated with 1 or 10 mM genipin or no genipin (control). All samples are measured in triplicate, and error bars represent standard deviations from the mean.

the cross-linking reaction. This incubation of acellular collagen hydrogels in solutions of genipin also causes the initially non-fluorescent samples to emit fluorescence in situ. When the collagen hydrogels exposed to genipin are subsequently excited with 590 nm light, the observed fluorescence emission maximum is a broad band with a peak centered at 630 nm (Figure 2A). The excitation of samples with different wavelengths of light produces very different fluorescence emission spectra (see the Supporting Information, Figure S1). Overall, cross-linking collagen hydrogels with 10 mM versus 1 mM genipin solution occurs faster and fluorescence levels off almost three times quicker. It reaches a plateau at ten hours after initiation of reaction (Figure 2B). However, both concentrations of genipin-treated collagen gels generate similar fluorescence intensity at 24 h. Therefore, as measured with fluorescence spectroscopy, the end point of modifying collagen gels with 1 mM and 10 mM genipin is the same. It implies that the 1 mM concentration of genipin that we use in this work is not a limiting factor in achieving a new equilibrium state representing the cross-linked collagen gels. It is potentially an important finding because 1 mM genipin can be directly applied to cross-link cell-containing collagen gels to strengthen their mechanical properties since cell exposure to this concentration of genipin causes only mild cytotoxicity.[26]

The fluorescence emission maximum detected at 630 nm (λ_{ex} = 590 nm) from the genipin-modified hydrogels is the same as observed in one other study[26] that used 590 nm light to excite genipin-modified collagen gels. An additional emission maximum that we detect at 464 nm (λ_{ex} = 300−400 nm) is similar to fluorescence emission at 469 nm observed by Chen et al.[31] from chitosan-genipin mixtures excited with 369 nm light. Our work and all previous relevant studies, therefore, suggest that cross-linking collagen hydrogels with genipin induces formation of multiple fluorophores. The formation of these different fluorophores is possibly due to different accessible amino acid residues within collagen reacting with genipin. The fluorescence emission maxima of these fluorophores depend strongly on the excitation wavelength.

In situ Microscopic Characterization of Genipin Cross-Linked Collagen Hydrogels: Second Harmonic Generation (SHG) and Fluorescence. To monitor the microstructures

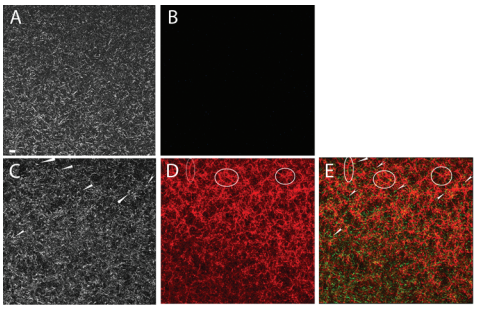

Figure 3. Typical fluorescence and second harmonic generation (SHG) images of a sample incubated with 1 mM genipin for a different amount of time. The images are taken in $X-Y$ plane. SHG, (A) 0 and (C) 48 h; fluorescence, (B) 0 and (D) 48 h; (E) merged fluorescence and SHG images. Formation of the long, aggregated strands with length longer than 20 μm can be seen in the fluorescence images within the areas circled with the white outline. The SHG generating collagen structures that remain after cross-linking with genipin are shown with arrows. The remaining SHG generating microstructures do not colocalize with the induced fluorescence. The collagen concentration of the sample is 2.0 mg/mL and the incubation temperature is 37 °C. The scale bar is 10 μm.

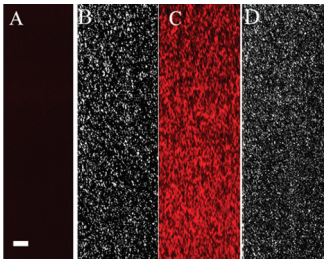

Figure 4. Typical fluorescence and second harmonic generation (SHG) images of a sample incubated with 1 mM genipin for a different amount of time. The images are taken in $X-Z$ plane. The collagen concentration is 2.0 mg/mL. The horizontal is the X-axis, and the vertical axis is the Z-axis. (A, C) Fluorescence; (B, D) SHG. (A, B) Control consisting of collagen only; (C, D) collagen hydrogel incubated with genipin. The scale is 20 μm. The top of each image represents the actual top of the imaged gel.

within collagen hydrogels during the cross-linking reaction with genipin, we employed LSM510 microscopy system equipped with both a Ti:Sapphire laser for SHG and a Helium−Neon 543 nm laser for fluorescence excitation.

To follow the extent of reaction during cross-linking collagen hydrogels with genipin, we excited samples with 543 nm light and followed the evolution of fluorescence intensity in the $x-y$ plane through the 565-615 nm filter (Figure 3B,D). When the cross-linking time reached 48 h, the structures exhibited high fluorescence intensity, and large fluorescent structures were formed (Figure 3D, white outline). The fluorescence images taken in $x-z$ plane showed that upon extended cross-linking (24 h or more) an increase of fluorescence occurred throughout the entire depth of collagen hydrogels (Figure 4C). The control group consisting of collagen hydrogels incubated in 0.3 M phosphate buffer saline solution did not exhibit detectable fluorescence (Figure 4A).

To determine if there are changes to the "fiberlike" microstructures within collagen hydrogels that are caused by cross-linking with genipin, we acquired second harmonic generation (SHG) images at the same time as fluorescence images. To the best of our knowledge, we are the first group to apply SHG and fluorescence imaging to carry out such evaluations. As seen in SHG images (Figure 3A,C), genipin cross-linking somewhat alters the microstructure of collagen hydrogels. Prior to the cross-linking, the "fiberlike" structures within the collagen hydrogels were short with lengths around 5−10 μm (Figure 3A). When the cross-linking time was 48 h, the short "fiberlike" SHG generating structures appeared "washed out" (Figure 3C) likely because of lowered intensity of SHG signal associated with them (unpublished data). The fibers did not undergo a radical change in appearance and did not duplicate the changes observed in fluorescence images.

The SHG images taken in $X-Z$ planes also showed that the observed homogenization of SHG generating collagen structures was throughout the entire depth of collagen hydrogels. This created an appearance of an increase in the density of now smaller "fiberlike" collagen structures (Figure 4D). On the basis of our previous studies, the strength of the detected backscattered SHG signals depends on the number of interfaces present in the assembled 'fiber-like' microstructures within collagen hydrogels.[23] Considering that the remaining SHG generating structures (arrows in Figure 3C) were not colocalized with cross-link derived fluorescence (Figure 3E), we speculate that the intra- and intermolecular cross-linking of collagen molecules by genipin partially disaggregated "fiberlike" collagen microstructures. We would expect that disaggregation diminishes the SHG contrast and furnishes dull appearance to the remaining SHG generating structures. The control group consisting of collagen hydrogels incubated in 0.3 M phosphate buffer saline did not have any structural changes that could be identified in the SHG images (Figure 4B).

The combination of fluorescence and SHG images presented in our work clearly show that genipin cross-linking does remodel the microscopic architecture within collagen hydrogels. By non-invasively sampling the structures within these mechanically stabilized templates employed in tissue engineering we reconstructed their overall 3D architecture. This reconstruction validates and confirms previous studies that recorded structural changes within various genipin cross-linked collagen-based tissues and materials. For example, when electrospun gelatin scaffolds were exposed to genipin, the morphology of preformed fibers was not maintained as detected with scanning electron microscopy.[32] Histological investigations revealed an increase in the fiber density and a decrease in interfibrillar spaces when corneas were treated with genipin.[33] When collagen/chitosan scaffolds were incubated with genipin, scanning electron microscopy studies showed the change of the pores' morphologies and sizes.[34] A recent study also showed that the pore size of genipin cross-linked collagen/chitosan scaffold became larger as observed with scanning electron microscopy.[35] However, another scanning electron microscopy study showed the decrease of pore size within the genipin cross-linked collagen−chondroitin sulfate−hyaluronic acid hybrid hydrogels.[36] The decrease in pore size was also noted for the electrospun silk fibroin/hydroxybutyl chitosan materials cross-linked with genipin as observed with scanning electron microscopy.[37]

To the best of our knowledge, we are the first to describe genipin-induced remodeling of collagen microstructures within 3D hydrogels and to directly link these changes to the induced fluorescence. Interestingly, during our study we additionally discovered that the 100 W mercury lamp emission filtered through the bandpass filter with a band center about 365 nm and bandwidth 50 nm would induce fluorescence. Specifically,

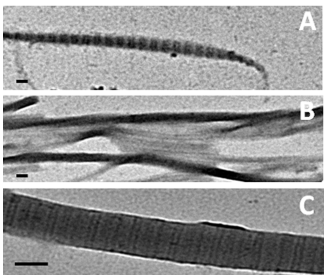

Figure 5. Transmission electron micrographs of negatively stained collagen fibrils cross-linked with genipin. (A) Typical collagen fibril with native banding. (B) Typical non-striated filaments. (C) Striated fibrils with non-native banding (longer D-period striation). The scale bar is 50 nm.

the areas of samples illuminated for several seconds with this lamp through the focusing objective, showed a strong enhancement in fluorescence intensity. However, we observed no corresponding change in the hydrogels' microstructure as detected with second harmonic generation (SHG) imaging (see the Supporting Information, Figure S2). The induced fluorescence dissipated within about fifteen minutes. We therefore concluded that this induced spectrally overlapping fluorescence is not associated with the formation of cross-links during reaction of collagen hydrogels with a genipin compound. It is possible that the fluorescent adducts of genipin itself are generated photochemically by UV light.

The structural analysis method that relies on fluorescence contrast as applied in this study is generally suitable for any cross-linked biomaterial in which cross-linking results in the formation of fluorescent structures. Therefore, genipin modified biopolymers chitosan, fibronectin, which contain primary amine groups as well as amniotic membrane are all acceptable test subjects. The materials that are non-centrosymmetric over macroscopic distances like the assembled collagen hydrogels used in this work can be investigated with second harmonic generation (SHG) signals as a source of contrast. The general utility of the SHG structural analysis method includes an ability to determine the sizes of collagen fibrils/fibers, their distribution and organization at depth within the scattering substrates such as collagen hydrogels examined in this work. We effectively applied a combination of the above contrasts to investigate the glycated[38] and EDC cross-linked (unpublished data) collagen hydrogels, collagen hydrogel-based models[39] as well as tissues.[40,41] The nondestructive structural analysis methods that rely on fluorescence and second harmonic generation contrasts resulting from electronic transitions and nonlinear interactions respectively provide complementary information to Raman and Fourier transform-based infrared techniques, which identify the molecular vibrations of the structural repeat units within biomaterials.

Characterization of Genipin Cross-Linked Collagen Hydrogels with Transmission Electron Microscopy. We used transmission electron microscopy to determine if in addition to affecting collagen microstructures, genipin modifies nanostructures as well. The transmission electron micrographs showed that the nanostructure of negatively stained reconstituted collagen fibrils varied greatly after treatments with genipin. Only under rare conditions, we observed native-like striated collagen fibrils with D-periods in the range of 62 to 67 nm (Figure 5A). Most of collagen fibrils became modified to non-striated filaments (Figure 5B). Additionally, we observed some striated fibrils with longer D-periods (Figure 5C). The genipin cross-linking mechanism depicted in Figure 1 could explain occurrence of non-native collagen structures in TEM images. The non-striated filaments and fibrils with non-native D-periods would form when there is a disruption of native staggered alignment of collagen molecules within fibrils. The intra- and inter-molecular cross-linking of collagen molecules by genipin likely induces this disruption.

Genipin compound is potentially an excellent natural cross-linking reagent for tissue engineering applications due to its low cytotoxicity and high cytocompatibility. For example, when Chang et al.[7] used genipin cross-linked gelatin membrane as a wound dressing material, he found that the inflammation was less severe and the healing rate was faster compared to using a glutaraldehyde-treated gelatin membrane. Yao et al.[9] applied genipin treated materials as bone substitutes and showed that they supported growth of a new bone without inflammation. Chen et al.[31] evaluated peripheral nerve regeneration using genipin-treated gelatin and found that this material led to an adequate nerve regeneration and functional recovery. Additionally, several researchers identified that genipin treated tissues and scaffolds support cellular viability, adhesion, and proliferation while preserving cellular activities and function.[4243]

The focus of this manuscript is on describing genipin-induced modifications of collagen micro- and nano- structures as well as optical spectral properties within 3D collagen hydrogels. However, our findings carry very broad implications. The optical methods we developed, describe cohesively the optical spectral properties for the reaction products between collagen and a genipin compound. In addition to aiding the development of collagen hydrogel standardization protocols for tissue engineering applications, our work can lead to a better understanding of the in situ reactions between a genipin compound and proteins. It will also possibly enhance and/or move forward the applications of genipin in various fields.

CONCLUSIONS

Collagen hydrogels have been cross-linked with a genipin compound and investigated with one-photon fluorescence spectroscopy, second harmonic generation, fluorescence and transmission electron microscopy. Genipin modification of collagen induces strong autofluorescence within hydrogels with emission maximum being dependent on the excitation wavelength. The emission maximum is observed at 630 nm when we excite the cross-linked samples with 590 nm light and shifts to 590 or 462 nm when we instead use 543 nm or 400 nm light respectively. The fluorescence imaging studies show that genipin induces formation of longer than 20 μm aggregated fluorescent strands throughout the depth of samples. The second harmonic generation (SHG) imaging studies suggest that genipin partially disaggregates 10 μm "fiberlike" collagen structures due to the formation of fluorescent cross-links. The transmission electron microscopy imaging further shows that the majority of native striated fibrils change to non-striated filaments or fibrils with non-native striation patterns. The kinetic studies indicate that even at 1 mM concentrations, genipin is not a limiting reagent. The amount of product formed is the same for 1 mM versus 10 mM genipin solutions and at 24 h post initiation of glycation there is no principle difference in the type of micro- or nanostructures formed. The knowledge obtained through this work provides us with a better understanding how to monitor the

extent of cross-linking of tissues and biologically derived scaffolds with a genipin reagent.

■ ASSOCIATED CONTENT

Supporting Information. Figure S1, the dependence of one-photon fluorescence emission spectrum of the genipin-modified collagen hydrogels on the excitation wavelength; Figure S2, an additional, induced spectrally overlapping fluorescence that was observed in this work. This fluorescence is not associated with the formation of cross-links during reaction of collagen hydrogels with a genipin compound. This fluorescence dissipates within about fifteen minutes. This material is available free of charge via the Internet at http://pubs.acs.org/.

■ AUTHOR INFORMATION

Corresponding Author
*E-mail: julial@ucr.edu.

■ ACKNOWLEDGMENT

The authors thank Prof. Jiayu Liao for access to the FlexStation fluorescence microplate reader (Molecular Devices) at UC Riverside. We thank Yong Song for the technical expertise and initial assistance with FlexStation. We thank Dr. Krassimir N. Bozhilov and Stephen McDaniel for the technical expertise with TEM at UC Riverside. We also thank Prof. Bruce J. Tromberg for access to a Zeiss LSM 510 NLO Meta microscopy system supported under the Laser Microbeam and Medical Program (LAMMP), a NIH Biomedical Technology Resource, Grant P41-RR01192. The work was supported by the UC Riverside startup research funds (J.G.L.) and the NSF CAREER Award CBET-0847070, NSF BRIGE Award EEC-0927297 (J.G.L.).

■ REFERENCES

(1) Sung, H.; Chang, Y.; Chang, W.; Chen, Y. *J. Biomed. Mater. Res.* **2000**, *52*, 77–87.
(2) Sung, H.; Huang, D.; Chang, W.; Huang, R.; Hsu, J. *J. Biomed. Mater. Res.* **1999**, *46*, 520–530.
(3) Lee, S.; Lim, J.; Bhoo, S.; Paik, Y.; Hahn, T. *Anal. Chim. Acta* **2003**, *480*, 267–274.
(4) Almog, J.; Cohen, Y.; Azoury, M.; Hahn, T. *J. Forensic Sci.* **2004**, *49*, 255–257.
(5) Levinton-Shamuilov, G.; Cohen, Y.; Azoury, M.; Chaikovsky, A.; Almog, J. *J. Forensic Sci.* **2005**, *50*, 1367–1371.
(6) Chen, Y. S.; Chang, J. Y.; Cheng, C. Y.; Tsai, F. J.; Yao, C. H.; Liu, B. S. *Biomaterials* **2005**, *26*, 3911–3918.
(7) Chang, W.; Chang, Y.; Lai, P.; Sung, H. *J. Biomater. Sci.* **2003**, *14*, 481–495.
(8) Chen, S. C.; Wu, Y. C.; Mi, F. L.; Lin, Y. H.; Yu, L. C.; Sung, H. W. *J. of Controlled Release* **2004**, *96*, 285–300.
(9) Yao, C. H.; Liu, B. S.; Hsu, S. H.; Chen, Y. S. *Biomaterials* **2005**, *26*, 3065–3074.
(10) Hanson, K. M.; Bardeen, C. J. *Photochem. Photobiol.* **2009**, *85*, 33–44.
(11) Yeh, A. T.; Nassif, N.; Zoumi, A.; Tromberg, B. J. *Opt. Lett.* **2002**, *27*, 2082–2084.
(12) Zipfel, W. R.; Williams, R. M.; Christie, R.; Nikitin, A. Y.; Hyman, B. T.; Webb, W. W. *Proc. Natl. Acad. Sci. U.S.A.* **2003**, *100*, 7075–7080.
(13) Raub, C. B.; Suresh, V.; Krasieva, T.; Lyubovitsky, J.; Mih, J. D.; Putnam, A. J.; Tromberg, B. J.; George, S. C. *Biophys. J.* **2006**, *92*, 2212–2222.
(14) Brown, E.; McKee, T.; DiTomaso, E.; Pluen, A.; Seed, B.; Boucher, Y. *Nat. Med.* **2003**, *9*, 796–801.
(15) Campagnola, P. J.; Millard, A. C.; Terasaki, M.; Hoppe, P. E.; Malone, C. J.; Mohler, W. A. *Biophys. J.* **2002**, *82*, 493–508.
(16) Guo, Y.; Savage, H. E.; Liu, F.; Schantz, S. P.; Ho, P. P.; Alfano, R. R. *Proc. Natl. Acad. Sci. U.S.A.* **1999**, *96*, 10854–10856.
(17) Masters, B. R.; So, P. T. C. *Microsc. Res. Tech.* **2004**, *63*, 3–11.
(18) Moreaux, L.; Sandre, O.; Charpack, S.; Blanchard-Desce, M.; Mertz, J. *Biophys. J.* **2001**, *80*, 1568–1574.
(19) Schenke-Layland, K.; Riemann, I.; Damour, O.; Stock, U. A.; Konig, K. *Advance Drug Delivery Reviews* **2006**, *58*, 878–896.
(20) Williams, R. M.; Zipfel, W. R.; Webb, W. W. *Biophys. J.* **2005**, *88*, 1377–1386.
(21) Zipfel, W. R.; Williams, R. M.; Christie, R.; Nikitin, A. Y.; Hyman, B. T.; Webb, W. W. *Proc. Natl. Acad. Sci. U.S.A.* **2003**, *100*, 7075–7080.
(22) Legare, F.; Pfeffer, C.; Olsen, B. R. *Biophys. J.* **2007**, *93*, 1312–1320.
(23) Hwang, Y.; Lyubovitsky, J. *Anal. Methods* **2011**, *3*, 529–536.
(24) Roth, S.; Freund, I. *J.Chem. Phys.* **1979**, *70*, 1637–1643.
(25) Chen, H.; Ouyang, W.; Lawuyi, B.; Martoni, C.; Prakash, S. *J. Biomed. Mater. Res.* **2005**, *75A*, 917–927.
(26) Sundararaghavan, H. G.; Monteior, G. A.; Lapin, N. A.; Chabal, Y. J.; Miksan, J. R.; Shreiber, D. I. *J. Biomed. Mater. Res.* **2008**, *87A*, 308–320.
(27) Bultier, M. F.; Ng, Y.; Pudney, P. D. A. *J. Polym. Sci., Part A: Poly. Chem.* **2003**, *41*, 3941–3953.
(28) Sung, H.; Huang, R.; Huang, L. H.; Tsai, C.; Chiu, C. *J. Biomed. Mater. Res.* **1998**, *42*, 560–567.
(29) Sung, H.; Liang, I.; Chen, C.; Huang, R.; Liang, H. *J. Biomed. Mater. Res.* **2001**, *55*, 538–546.
(30) Fujikawa, S.; Fukui, Y.; Koga, K.; Kumada, J. *J. Ferment. Technol.* **1987**, *65*, 419–424.
(31) Chen, H.; Ouyang, W.; Lawuyi, B.; Martioni, C.; Prakash, S. *J. Biomed. Mater. Res.* **2005**, *75A*, 917–927.
(32) Sisson, K.; Zhang, C.; Farach-Carson, M. C.; Chase, D. B.; Rabolt, J. F. *Biomacromolecules* **2009**, *10*, 1675–1680.
(33) Avila, M. Y.; Navis, J. L. *J. Cataract Refract. Surg.* **2010**, *36*, 659–664.
(34) Yan, L.; Wang, Y.; Ren, L.; Wu, G.; Caridade, S. G.; Fan, J.; Wang, L.; Ji, P.; Oliverira, J. M.; Mano, J. F.; Reis, R. L. *J. Biomed. Mater. Res.* **2010**, *95A*, 465–475.
(35) Bi, L.; Cao, Z.; Hu, Y.; Song, Y.; Yu, L.; Yang, B.; Mu, J.; Huang, Z.; Han, Y. *J. Mater. Sci. : Mater. Med.* **2011**, 51–62.
(36) Zhang, Z.; Li, K.; Xiao, W.; Zheng, L.; Xiao, Y.; Fan, H.; Zhang, X. *Carbo. Poly.* **2011**, *84*, 118–125.
(37) Zhang, K.; Qian, Y.; Wang, H.; Fan, L.; Huang, C.; Yin, A.; Mo, X. *J. Biomed. Mater. Res* **2010**, *95A*, 870–881.
(38) Hwang, Y.; Granelli, J.; Lyubovitsky, J. *Anal. Chem.* **2011**, *83*, 200–206.
(39) Hwang, Y.; Kolletis, N.; Yang, M.; Sanchez, E., '; Sun, C.; Gillard, E. R.; Tromberg, B. J.; Krasieva, T. B.; Lyubovitsky, J. G. *Photochem. Photobiol.* **2010**, DOI: 10.1111/j.1751-1097.2010.00873.x.
(40) Lyubovitsky, J. G.; Krasieva, T. B.; Spencer, J. A.; Andersen, B.; Tromberg, B. J. *J. Biomed. Optics* **2005**, *11*, 014013.
(41) Lyubovitsky, J. G.; Krasieva, T. B.; Xu, X.; Andersen, B.; Tromberg, B. J. *J. Biomed. Opt.* **2007**, *12*, 044003.
(42) Yu, X.; Liu, F.; Xu, Y.; Wang, C. *J. Mater. Sci: Mater. Med.* **2010**, *21*, 777–785.
(43) Lau, T.; Wang, C.; Png, S.; Su, K.; Wang, D. *J. Biomed. Mater. Res.* **2011**, *96A*, 204–211.